Delay-Dependent Stability for Load Frequency Control System via Linear Operator Inequality

Changchun Hua, *Senior Member, IEEE*, and Yibo Wang

***Abstract*—The stability analysis problem is considered for multiarea load frequency control (LFC) systems with electric vehicles (EVs) and time delays. The novel linear operator inequality approach is proposed and a less conservative delay-dependent stability condition is achieved. First, the model of the multiarea LFC system with EVs and delays is expressed by the partial integral equation (PIE) at the first time. Then, a complete quadratic Lyapunov–Krasovskii functional is built in the form of an inner product of the linear partial integral (PI) operator. The novel stability criteria with less conservatism are proposed in the form of linear operator inequality. Moreover, the relationships between the delay margins and the controller parameters are shown. Finally, the simulations are conducted on both one-area and two-area LFC systems to show the effectiveness of the proposed approach.**

***Index Terms*—Complete quadratic Lyapunov–Krasovskii functional, delay-dependent stability, load frequency control (LFC), time delay.**

I. Introduction

THE STABILITY of the load frequency is one of the important indicators to evaluate the power system. The load frequency control (LFC) system is introduced to maintain the frequency stability of the power system as in [1] and [2]. Time delay is a prevalent problem in the LFC system due to: 1) more open communication network being adopted to provide efficient bilateral communication; 2) existence of a geographically distributed power area; 3) cyber attack causes time delay in the control signal; and 4) the penetration of distributed generators and renewable energy generation as in [3]. The existence of time delay would degrade the performance of the LFC system or even destabilize the LFC system. Therefore, it is essential to study the delay-dependent stability of the LFC system with time delay.

In the last few decades, the studies on the LFC system with electric vehicles (EVs) have gained much attention. In [4], an H_∞ control scheme was designed to guarantee the stability of the LFC system with state of charge (SOC) control. Tian and Peng [5] proposed a memory H_∞ controller for a one-area LFC system with EVs under deception attacks. The LFC system with EVs was investigated by using the event-triggered control approach in [6]. The problem of stability of a one-area LFC system with EV aggregator and time delay was investigated in [7]. The participation of EVs in the LFC system is conducive to suppress system frequency fluctuations caused by load disturbances. The purpose of this article is to study the delay-dependent stability of the multiarea LFC system with EVs and time delays.

The delay differential equations (DDEs) are normally used to describe the system with time delay. Therefore, the LFC scheme with the open communication network is regarded as a common time-delay system represented by DDEs, which can be found in [8]–[15]. The purpose of studying the delay-dependent stability of LFC system is to obtain a less conservative stability condition, which can accurately estimate the boundary of the time delay. The frequency-domain method (see [7], [16], and [17]) can acquire the accurate delay margins by calculating the eigenvalues of the system, but it may be not suitable for the multiarea LFC system with uncertainties. In order to reduce conservatism, an enormous amount of research in the last decade has focused on constructing a simple L—K functional, such as standard L–K functional [18], augmented L–K functional [19], and functional with triple-integral term [20]. In [18], one-area and multiarea LFC systems were studied to acquire the relationships between delay margins and controller parameters by using the standard L-K functional. Based on the result in [18], Zhang *et al.* [21] further examined the connection between gains of controller and time delays, and the interactions among different areas based on augmented functional. An augmented functional was developed in [22] to discuss the stability problem for a partial integral (PI)-type LFC system with time-varying delay. In [23], the multiarea LFC system with time delays was investigated by employing an augmented L–K functional with triple integral terms. In summary, numerous methods have been developed to diminish the conservatism for stability analysis of the LFC system. However, a simple L–K functional may not contain the complete information of the system, which inevitably leads to the conservativeness of the criterion. The purpose of this article is to propose a more general L–K functional for the stability analysis of the multiarea LFC system with EVs and time delays.

Another source of conservatism is to constrain the cross terms appearing in the simple L–K functional derivation. In [24], the Jenson integral inequality was utilized to generate a less

Manuscript received 27 April 2020; revised 29 August 2020; accepted 28 October 2020. Date of publication 11 December 2020; date of current version 1 July 2022. This work was supported in part by the National Key Research and Development Program of China under Grant 2018YFB1308304; and in part by the National Natural Science Foundation of China under Grant 61825304, Grant 61751309, and Grant 61673335. This article was recommended by Associate Editor T. H. Lee. *(Corresponding author: Changchun Hua.)*

The authors are with the School of Electrical Engineering, Yanshan University, Qinhuangdao 066004, China (e-mail: cch@ysu.edu.cn; wyb13032317@foxmail.com).

Color versions of one or more figures in this article are available at https://doi.org/10.1109/TCYB.2020.3037113.

Digital Object Identifier 10.1109/TCYB.2020.3037113

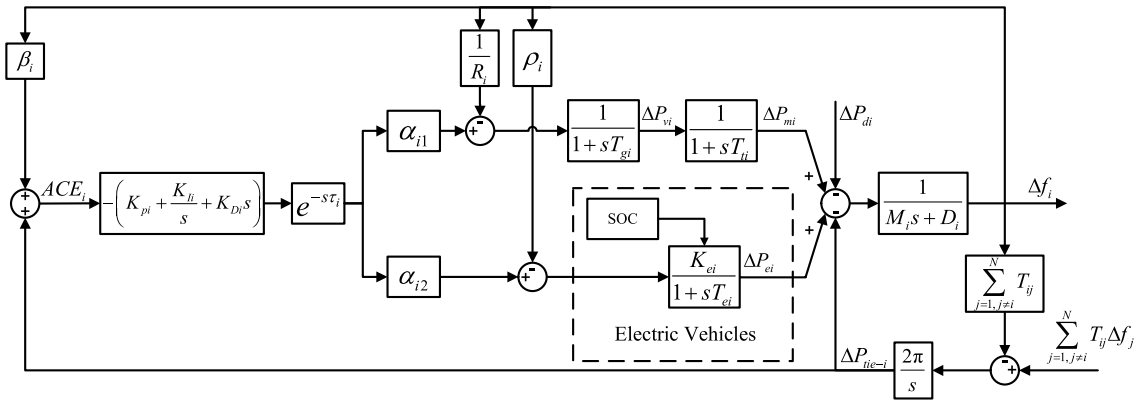

Fig. 1. Structure of multiarea LFC system with EVs and time delays.

conservative stability condition for the LFC system with time delay. The stability problem of the LFC system with sampling and transmission delay was studied by using the Wirtinger inequality in [25]. Yang *et al.* [13] established a stability condition by means of the B-L inequality for the LFC system with time delay and nonlinear disturbances. A discrete LFC system with wind power was investigated based on sampled-data control in [14]. The model reconstruction method, combined with the Wirtinger inequality, was utilized to obtain stability criteria with low computational complexity in [26]. Hua *et al.* [27] investigated the problem of delay-dependent stability of the microgrid frequency control system by employing the auxiliary function-based integral inequality that encompasses the Wirtinger inequality. Although the integral inequality can be employed to deal with cross terms, it may make the criterion more conservative. Recently, based on semigroup theory and linear operator theory, Peet [28] proposed a class of linear PI operators. Moreover, the MATLAB toolbox PIETOOLS was proposed in the sum of squares (SOS) framework, which can efficiently construct and process a PI operator (see [29] and [30]). To diminish the effect of integral inequality, this article introduced the operator inequality method into the stability analysis of LFC system.

In this article, the delay-dependent stability of multiarea LFC system with EVs and time delays was investigated based on linear operator inequality. It is worth noting that the contributions of this article are as follows.

1) The multiarea LFC system with EVs and time delays was represented by the PI equation (PIE) for the first time in this article, which can represent the dynamics of the system and reduce the complexity of stability analysis.
2) A complete quadratic L–K functional was built in the form of an inner product of the PI operator, which has the potential to obtain accurate stability conditions.
3) The novel stability criteria for the multiarea LFC systems with time delays were proposed in this article, which were less conservative than existing literature. Furthermore, the relationships between controller parameters and delay margins were further studied.

Notation: $\mathbb{R}^n$ denotes the n-dimensional real Euclidean space. $\mathbb{R}^{n\times m}$ represents the set of all $n \times m$ real matrices. For a normed space X, $L_2^m := L_2(X;\mathbb{R}^n)$ denotes the Hilbert space of square integrable functions from X to $\mathbb{R}^m$ and we define $W_2^m[X] := \{x : x, \dot{x} \in L_2^m[X]\}$. $Z := Z_{n,m}$ denotes the inner product space $\mathbb{R}^n \times L_2^m[-1, 0]$. The operator $\mathcal{P} : Z \to Z$ is positive if $\langle x, \mathcal{P}x\rangle_Z \geq 0$ for all $x \in X$, where X is a subset of Z. $\mathcal{P}^*$ is the adjoint operator of $\mathcal{P}$. For any $x \in Z$, $y \in Z$, $\langle x, y\rangle_Z = \int_X x^{\mathrm{T}} y ds$. I and 0, respectively, represent the identity matrix and the zero matrix of appropriate dimensions. For a matrix P, $P > 0 (\geq 0)$ means that P is positive definite (semidefinite). P^{T} stands for the transposition of P. The symbol diag$\{\cdots\}$ represents a block-diagonal matrix.

The remainder of this article is arranged as follows. Section II presents the multiarea LFC system with time delays expressed by PIE. Section III provides the delay-dependent stability criteria for multiarea LFC system and the corresponding algorithm. In Section IV, case studies are conducted. The conclusion is proposed in Section V.

II. Dynamic Model and Preliminary

In this section, the state space model of the multiarea LFC scheme with EVs and time delays is reviewed at first. Then, the PI operator is introduced to convert the original model of the LFC system to the system expressed by PIE representation.

A. ODE Representation

The classical LFC structure represented by ODEs in [4] has been developed in this section, in which each area contains EVs with the SOC and PID controller. Fig. 1 shows the structure of i area in the multiarea LFC system, where ΔP_{vi}, ΔP_{di}, ΔP_{mi}, and Δf_i denote the valve position, disturbance of load, the mechanical output of the generator unit, and deviation of frequency, respectively; τ_i is the time delay encountered between the controller and the actuator. M_i and D_i are the inertia constant and damping coefficient of the generator unit, respectively; T_{gi} and T_{ti} denote the time constant of the generator unit and turbine, respectively; R_i and β_i are speed droop and frequency bias factor, respectively; T_{ij} is the synchronizing coefficient of tie-line; and α_{i1} and α_{i2} denote the participation factors of generators. T_{ei} is the time constant of the first-order model of EV; and N refers to the N areas contained in the LFC system.

As in [4], EVs with and without SOC are both considered in the LFC system. The gain K_{ei} of EV in area i is as follows:

$$K_{ei} = \bar{K}_{ei} - \eta \bar{K}_{ei} g(t) \tag{1}$$

where η is the ratio of EVs with SOC, and $g(t)$ is a function satisfying $0 \le g(t) \le 1$.

The traditional LFC state space model of area i can be obtained

$$\begin{aligned}\dot{x}_i(t) &= (A_i + \Delta A_i)x_i(t) + \sum_{j=1, j\neq i}^{N} A_{ij}x_j(t) \\ &\quad + (B_i + \Delta B_i)u_i(t-\tau_i) + F_i \Delta P_{di}(t) \\ y_i(t) &= C_i x_i(t)\end{aligned} \tag{2}$$

where

$$\begin{aligned}x_i(t) &= \begin{bmatrix}\Delta f_i & \Delta P_{\text{tie}-i} & \Delta P_{mi} & \Delta P_{vi} & \Delta P_{ei}\end{bmatrix}^{\mathrm{T}} \\ y_i(t) &= ACE_i(t) \\ A_i &= \begin{bmatrix} -\frac{D_i}{M_i} & -\frac{1}{M_i} & \frac{1}{M_i} & 0 & \frac{1}{M_i} \\ 2\pi \sum_{j=1, j\neq i}^{N} T_{ij} & 0 & 0 & 0 & 0 \\ 0 & 0 & -\frac{1}{T_{ti}} & \frac{1}{T_{ti}} & 0 \\ -\frac{1}{T_{gi}R_i} & 0 & 0 & -\frac{1}{T_{gi}} & 0 \\ -\frac{\rho_i \bar{K}_{ei}}{T_{ei}} & 0 & 0 & 0 & -\frac{1}{T_{ei}} \end{bmatrix} \\ \Delta A_i^{\mathrm{T}} &= \begin{bmatrix} 0 & 0_{1\times 4} \\ 0 & 0_{1\times 4} \\ 0 & 0_{1\times 4} \\ 0 & 0_{1\times 4} \\ \frac{\rho_i \bar{K}_{ei}\eta g(t)}{T_{ei}} & 0_{1\times 4} \end{bmatrix}, \ A_{ij} = \begin{bmatrix} 0 & 0_{1\times 4} \\ -2\pi T_{ij} & 0_{1\times 4} \\ 0 & 0_{1\times 4} \\ 0 & 0_{1\times 4} \\ 0 & 0_{1\times 4} \end{bmatrix} \\ B_i^{\mathrm{T}} &= \begin{bmatrix} 0 & 0 & 0 & \frac{\alpha_{i1}}{T_{gi}} & \frac{\alpha_{i2}\bar{K}_{ei}}{T_{ei}} \end{bmatrix} \\ \Delta B_i^{\mathrm{T}} &= \begin{bmatrix} 0 & 0 & 0 & 0 & -\frac{\eta \bar{K}_{ei}\alpha_{i2} g(t)}{T_{ei}} \end{bmatrix} \\ F_i^{\mathrm{T}} &= \begin{bmatrix} -\frac{1}{M_i} & 0 & 0 & 0 & 0 \end{bmatrix} \\ C_i &= \begin{bmatrix} \beta_i & 1 & 0 & 0 & 0 \end{bmatrix}.\end{aligned}$$

In order to facilitate analysis, the static output feedback strategy is utilized to investigate the PID control problem. A PID controller for area i is provided with $K_i = [K_{Pi}, K_{Ii}, K_{Di}]$.

The closed-loop system of i area LFC scheme with EVs and time delays is established as

$$\begin{aligned}\dot{\hat{x}}_i &= \left(\hat{A}_{ii} + \Delta\hat{A}_{ii}\right)\hat{x}_i(t) + \left(\hat{A}_{dii} + \Delta\hat{A}_{dii}\right)\hat{x}_i(t-\tau_i) \\ &\quad + \sum_{j=1, j\neq i}^{N} \left(\hat{A}_{ij}\hat{x}_j(t) + \left(\hat{A}_{dij} + \Delta\hat{A}_{dij}\right)\hat{x}_j(t-\tau_i)\right) \\ &\quad + \hat{F}_i \Delta P_{di}(t)\end{aligned} \tag{3}$$

where

$$\begin{aligned}\hat{A}_{ii} &= \begin{bmatrix} A_i & 0 \\ C_i & 0 \end{bmatrix}, \ \Delta\hat{A}_{ii} = \begin{bmatrix} \Delta A_i & 0 \\ 0 & 0 \end{bmatrix}, \ \hat{A}_{ij} = \begin{bmatrix} A_{ij} & 0 \\ 0 & 0 \end{bmatrix} \\ \Delta\hat{A}_{dii} &= -\Delta\hat{B}_i K_i \hat{C}_i, \ \Delta\hat{A}_{dij} = -\Delta\hat{B}_i K_i \hat{C}_{ij} \\ \hat{A}_{dii} &= -\hat{B}_i K_i \hat{C}_i, \ \hat{A}_{dij} = -\hat{B}_i K_i \hat{C}_{ij} \\ \hat{F}_i &= \bar{F} - \hat{B}_i K_i \hat{D}_i - \Delta\hat{B}_i K_i \hat{D}_i, \ \bar{F}^{\mathrm{T}} = \begin{bmatrix} F_i^{\mathrm{T}} & 0 \end{bmatrix} \\ \hat{B}_i^{\mathrm{T}} &= \begin{bmatrix} B_i & 0 \end{bmatrix}, \ \Delta\hat{B}_i^{\mathrm{T}} = \begin{bmatrix} \Delta B_i & 0 \end{bmatrix}\end{aligned}$$

$$\hat{C}_i = \begin{bmatrix} C_i & 0 \\ 0 & 1 \\ C_i A_i & 0 \end{bmatrix}, \ \hat{C}_{ij} = \begin{bmatrix} 0 & 0 \\ 0 & 0 \\ C_i A_{ij} & 0 \end{bmatrix}, \ \hat{D}_i = \begin{bmatrix} 0 \\ 0 \\ C_i F_i \end{bmatrix}.$$

Finally, let the state vector be $x = [\hat{x}_1^{\mathrm{T}}, \ldots, \hat{x}_N^{\mathrm{T}}]^{\mathrm{T}}$, then the whole closed-loop multiarea LFC system is constructed as

$$\begin{aligned}\dot{x}(t) &= (A + \Delta A)x(t) + \sum_{i=1}^{N}(A_{di} + \Delta A_{di})x(t-\tau_i) \\ &\quad + F\Delta P_d(t)\end{aligned} \tag{4}$$

where

$$\begin{aligned}A &= \begin{bmatrix} \hat{A}_{11} & \cdots & \hat{A}_{1N} \\ \vdots & \ddots & \vdots \\ \hat{A}_{N1} & \cdots & \hat{A}_{NN} \end{bmatrix}, \ A_{di} = \begin{bmatrix} 0_{6(i-1)\times 6N} \\ \hat{A}_{di1}, \ldots, \hat{A}_{diN1} \\ 0_{6(N-i)\times 6N} \end{bmatrix} \\ \Delta A_{di} &= \begin{bmatrix} 0_{6(i-1)\times 6N} \\ \Delta\hat{A}_{di1}, \ldots, \Delta\hat{A}_{diN} \\ 0_{6(N-i)\times 6N} \end{bmatrix}, \ \Delta P_d(t) = \begin{bmatrix} \Delta P_{d1}(t) \\ \vdots \\ \Delta P_{dN}(t) \end{bmatrix}^{\mathrm{T}} \\ \Delta A &= \operatorname{diag}\left\{\Delta\hat{A}_{11}, \ldots, \Delta\hat{A}_{NN}\right\}, \ F = \operatorname{diag}\left\{\hat{F}_i, \ldots, \hat{F}_N\right\}.\end{aligned}$$

It must be noted that the net tie-line power exchange between areas satisfies $\sum_{i=1}^{N} \Delta P_{\text{tie}-i} = 0$. Therefore, $\Delta P_{\text{tie}-i}$ can be represented by $-\sum_{j=1, j\neq i}^{N} \Delta P_{\text{tie}-i}$.

According to the characteristics of the external disturbance, it will not affect the internal stability of the LFC system (see [6]). Therefore, the problem of stability analysis of multiarea LFC system with EVs and time delays can be considered as follows:

$$\dot{x}(t) = (A + \Delta A)x(t) + \sum_{i=1}^{N}(A_{di} + \Delta A_{di})x(t-\tau_i). \tag{5}$$

Remark 1: The multiarea LFC system with EVs and time delays is developed in this section. Compared with the model in [4], the multiarea LFC structure is established in this article. The EV model in [5] and [6] does not consider SOC, which can be regarded as a special form of the system in this article. Therefore, the LFC scheme investigated in this article is more general.

B. PIE Representation

In this section, the original model of the LFC system is converted to a system expressed by PIE representation. Before proposing the main results of this article, some lemmas are recalled in this section. First, the definition of PI operator is as follows.

Definition 1 [31]: The PI operator $\mathcal{P}\begin{bmatrix} P, & Q_1 \\ Q_2, & \{R_i\} \end{bmatrix} : \mathbb{R}^m \times L_2^n[-1, 0] \to \mathbb{R}^p \times L_2^q[-1, 0]$ satisfies the following condition:

$$\left(\mathcal{P}\begin{bmatrix} P, & Q_1 \\ Q_2, & \{R_i\} \end{bmatrix}\begin{bmatrix} x \\ \psi \end{bmatrix}\right)(s) := \begin{bmatrix} Px + \int_{-1}^{0} Q_1(s)\psi(s)ds \\ Q_2(s)x + \Xi(R_i, \psi) \end{bmatrix} \tag{6}$$

where $\Xi(R_i, \psi) = R_0(s)\psi(s) + \int_{-1}^{s} R_1(s, \eta)\psi(\eta)d\eta + \int_{s}^{0} R_2(s, \eta)\psi(\eta)d\eta$ and matrix $P \in \mathbb{R}^{p\times m}$, bounded polynomial functions $Q_1(s) \in W_2^{p\times n}[-1, 0]$, $Q_2(s) \in W_2^{q\times m}[-1, 0]$, $R_0(s) \in W_2^{q\times n}[-1, 0]$, $R_1(s, \eta), R_2(s, \eta) \in W_2^{q\times n}[[-1, 0] \times [-1, 0]]$.

As mentioned in [31], the PI operator is positive and self-adjoint. The PI operator can be parameterized by employing matrix-valued functions. The parameterization method of PI operator is as follows.

Lemma 1 [32]: For any polynomial matrix function $G_1 : [-1, 0] \to \mathbb{R}^{m_1 \times n}$, $G_2 : [-1, 0] \times [-1, 0] \to \mathbb{R}^{m_2 \times n}$ and function $f(s) \geq 0, s \in [-1, 0]$, if

$$\begin{aligned}
P &= S_{11} \int_{-1}^{0} f(s)ds \\
Q &= f(s)S_{12}G_1(s) + \int_{s}^{0} f(\eta)S_{13}G_2(\eta, s)ds \\
&\quad + \int_{-1}^{s} f(\eta)S_{14}G_2(\eta, s)ds \\
R_0(s) &= f(s)G_1^{\mathrm{T}}(s)S_{22}G_1(s) \\
R_1(s, \eta) &= f(s)G_1^{\mathrm{T}}(s)S_{23}G_2(s, \eta) + f(\eta)G_2^{\mathrm{T}}(\eta, s)S_{42}G_1(\eta) \\
&\quad + \int_{s}^{0} f(\theta)G_2^{\mathrm{T}}(\theta, s)S_{33}G_2(\theta, \eta)d\theta \\
&\quad + \int_{\eta}^{s} f(\theta)G_2^{\mathrm{T}}(\theta, s)S_{43}G_2(\theta, \eta)d\theta \\
&\quad + \int_{-1}^{\eta} f(\theta)G_2^{\mathrm{T}}(\theta, s)S_{44}G_2(\theta, \eta)d\theta \\
R_2(s, \eta) &= f(s)G_1^{\mathrm{T}}(s)S_{32}G_2(s, \eta) + f(\eta)G_2^{\mathrm{T}}(\eta, s)S_{24}G_1(\eta) \\
&\quad + \int_{\eta}^{0} f(\theta)G_2^{\mathrm{T}}(\theta, s)S_{33}G_2(\theta, \eta)d\theta \\
&\quad + \int_{s}^{\eta} f(\theta)G_2^{\mathrm{T}}(\theta, s)S_{34}G_2(\theta, \eta)d\theta \\
&\quad + \int_{-1}^{s} f(\theta)G_2^{\mathrm{T}}(\theta, s)S_{44}G_2(\theta, \eta)d\theta
\end{aligned}$$

where

$$S = \begin{bmatrix} S_{11} & S_{12} & S_{13} & S_{14} \\ S_{21} & S_{22} & S_{23} & S_{24} \\ S_{31} & S_{32} & S_{33} & S_{34} \\ S_{41} & S_{42} & S_{43} & S_{44} \end{bmatrix} \geq 0.$$

Then, the PI operator defined in (4) satisfies

$$\mathcal{P}\begin{bmatrix} P, & Q_1 \\ Q_2, & \{R_i\} \end{bmatrix} \geq 0. \tag{7}$$

Proof: The proof can be found in [32].

The following function is defined:

$$\psi_i(t, s) = x(t + s\tau_i), (s \in [-1, 0]). \tag{8}$$

Note that $\psi_i(t, s)$ can represent the ith historical state of the delay channel of system (5). Obviously, the following condition can be obtained by defining $s = 0$:

$$\psi_i(t, 0) = x(t). \tag{9}$$

By taking the derivative of $\psi_i(t, s)$ with respect to t and s, respectively, the following equality holds:

$$\psi_{it}(t, s) = \frac{1}{\tau_i}\psi_{\mathrm{is}}(t, s). \tag{10}$$

Equation (9) is the boundary condition and (10) is a differential condition.

We define

$$\psi(t, s) = \left[\psi_1^{\mathrm{T}}(t, s), \psi_2^{\mathrm{T}}(t, s), \ldots, \psi_N^{\mathrm{T}}(t, s)\right]^{\mathrm{T}} \tag{11}$$

where $\psi_i(t, s) = x(t + s\tau_i)$. The boundary condition and differential condition of $\psi(t, s)$ are as follows:

$$\psi(t, 0) = \bar{I}x(t) \tag{12}$$

$$\psi_t(t, s) = \Upsilon\psi_s(t, s) \tag{13}$$

where

$$\Upsilon = \mathrm{diag}\left\{\frac{1}{\tau_1}I, \ldots, \frac{1}{\tau_N}I\right\}, \ \bar{I} = \left[\underbrace{I, \ldots, I}_{N}\right]^{\mathrm{T}}.$$

Based on the basic calculus rules and (12), $\psi(t, s)$ is yielded

$$\begin{aligned}
\psi(t, s) &= \psi(t, 0) - \int_{s}^{0} \psi_s(t, \eta)d\eta \\
&= \bar{I}x(t) - \int_{s}^{0} \psi_s(t, \eta)d\eta.
\end{aligned} \tag{14}$$

By taking the derivative of (14) with respect to t, the following condition holds based on (13):

$$\bar{I}\dot{x}(t) - \int_{s}^{0} \dot{\psi}_s(t, \eta)d\eta = \Upsilon\psi_s(t, s). \tag{15}$$

It is worth noting that the boundary condition (12) and the differential condition (13) are unified in (15).

The function (8) can be written as follows when $s = -1$:

$$\psi_i(t, -1) = x(t - \tau_i). \tag{16}$$

Based on (14) and (16), the system (5) can be presented as

$$\begin{aligned}
\dot{x}(t) &= (A + \Delta A)x(t) + \sum_{i=1}^{N}(A_{di} + \Delta A_{di})x(t - \tau_i) \\
&= (A + \Delta A)x(t) \\
&\quad + \sum_{i=1}^{N}(A_{di} + \Delta A_{di})\left(x(t) - \int_{-1}^{0} \psi_{\mathrm{is}}(t, \eta)d\eta\right) \\
&= \bar{A}_0 x(t) - \int_{-1}^{0} \bar{A}_1\psi_s(t, s)ds \\
&\quad + \Delta\bar{A}_0 x(t) - \int_{-1}^{0} \Delta\bar{A}_1\psi_s(t, s)ds
\end{aligned} \tag{17}$$

where

$$\begin{aligned}
\bar{A}_0 &= A + \sum_{i=1}^{N} A_{di}, \bar{A}_1 = [A_{d1}, \ldots, A_{dN}] \\
\Delta\bar{A}_0 &= \Delta A + \sum_{i=1}^{N} \Delta A_{di}, \Delta\bar{A}_1 = [\Delta A_{d1}, \ldots, \Delta A_{dN}].
\end{aligned}$$

Inspired by the work of [31], the fundamental state $x_f = [x^{\mathrm{T}}(t), \psi_s^{\mathrm{T}}(t, s)]^{\mathrm{T}} \in Z_{n,nN}$ is defined. Based on (15) and (17), the LFC system (5) is rewritten as PDE-ODE coupling form as follows:

$$\begin{bmatrix} \dot{x}(t) \\ \bar{I}\dot{x}(t) - \int_s^0 \dot{\psi}_s(t,\eta)d\eta \end{bmatrix} = \begin{bmatrix} (\bar{A}_0 + \Delta\bar{A}_0)x(t) - \int_{-1}^0 (\bar{A}_1 + \Delta\bar{A}_1)\psi_s(t,s)ds \\ \Upsilon\psi_s(t,s) \end{bmatrix}. \quad (18)$$

Finally, by defining operators $\mathcal{T} : Z_{n,nN} \to Z_{n,nN}$ and $\mathcal{A} : Z_{n,nN} \to Z_{n,nN}$, the PDE-ODE coupled system can be directly converted into the PIE representation as follows:

$$\mathcal{T}\dot{x}_f(t) = \mathcal{A}x_f(t) \quad (19)$$

where

$$\mathcal{T} = \mathcal{P}\begin{bmatrix} I & 0 \\ \bar{I} & \{0,0,-I\} \end{bmatrix}, \ \mathcal{A} = \mathcal{P}\begin{bmatrix} \bar{A}_0 + \Delta\bar{A}_0 & \bar{A}_1 + \Delta\bar{A}_1 \\ 0 & \{\Upsilon,0,0\} \end{bmatrix}.$$

When $\psi(t,s)$ satisfies the boundary condition (12) and differential condition (13), the dynamics of the state $x(t)$ in system (19) is identical with the system (5). In other words, system equations (5) and (19) have the same solution $x(t)$. Therefore, the stability analysis problem of system (5) can be transformed into the stability of system (19) ■

Remark 2: The LFC system represented by PIE (19) has significant advantages over one represented by DDE (5). The primary advantage is that the LFC system (19) represented by PIE does not contain some implicit dynamics, such as $x(t-\tau_i)$. Because the system (19) defines implicit dynamics through boundary condition and state $\psi(t,s)$, which reduce the difficulty of system analysis. Furthermore, by employing the PIETOOLS, the LFC system expressed by PIE can be easily analysed and synthesized.

III. Stability Analysis for LFC

This section provides stability criteria and analysis procedures for multiarea LFC system expressed by PIE. First, a complete quadratic L–K functional is given and expressed in the form of PI operator. Then, based on the complete quadratic L–K functional, the stability criteria with less conservatism are proposed. Finally, the procedures for calculating the delay margin are given.

For the LFC system (5), the stability is equivalent to the existence of a complete quadratic L–K functional in the following form:

$$V(t) = \int_{-1}^0 \begin{bmatrix} x(t) \\ \psi(t,s) \end{bmatrix}^{\mathrm{T}} \begin{bmatrix} P & Q(s) \\ Q^{\mathrm{T}}(s) & S(s) \end{bmatrix} \begin{bmatrix} x(t) \\ \psi(t,s) \end{bmatrix} ds + \int_{-1}^0 \int_{-1}^0 \psi(t,s)^{\mathrm{T}} R(s,\theta)\psi(t,s)dsd\theta. \quad (20)$$

According to the definition of PI operator, (20) is easily written as

$$V(t) = \langle v, \mathcal{P}v\rangle_Z \quad (21)$$

where $v := \begin{bmatrix} x^{\mathrm{T}} & \psi^{\mathrm{T}}(t,s) \end{bmatrix}^{\mathrm{T}}$, $\mathcal{P} := \mathcal{P}\begin{bmatrix} P & Q \\ Q & \{S,R,R\} \end{bmatrix}$.

Remark 3: The complete quadratic L–K functional is more general than simple L–K functional. It is worth noting that the parameters $Q(s)$, $S(s)$, and $R(s,\theta)$ in the complete quadratic L–K functional (20) are all matrix functions. The parameters, however, in simple L–K functional are all matrices. Therefore, the complete quadratic L–K functional has the potential to obtain an accurate stability condition. However, it is worth noting that the complete quadratic L–K functional may lead to a high computational complexity. Then, for the system (19), the stability criteria are obtained as follows.

Theorem 1: For given time delays $\tau_i (i = 0, 1, \ldots, N)$ and $g(t) \in \{0, 1\}$, the system (19) is asymptotically stable if there exist a positive, self-adjoint PI operator $\mathcal{P} := \mathcal{P}\begin{bmatrix} P, & Q_1 \\ Q_2, & \{R_i\} \end{bmatrix}$ such that the following inequality holds:

$$\mathcal{T}^*\mathcal{P}(\mathcal{A}_1 + g(t)\mathcal{A}_2) + (\mathcal{A}_1 + g(t)\mathcal{A}_2)^*\mathcal{P}\mathcal{T} < 0. \quad (22)$$

Proof: The complete quadratic L–K functional candidate is established as follows:

$$V(x_f) = \langle \mathcal{T}x_f, \mathcal{P}\mathcal{T}x_f\rangle_Z. \quad (23)$$

Due to the PI operator $\mathcal{P}$ is positive-definite operator, $V(x_f) \geq \varepsilon\|x_f\|^2$ is satisfied for any ε.

Then, the calculation of $\dot{V}(x_f)$ gives

$$\begin{aligned} \dot{V}(x_f) &= \langle \mathcal{T}x_f, \mathcal{P}\mathcal{A}x_f\rangle_Z + \langle \mathcal{A}x_f, \mathcal{P}\mathcal{T}x_f\rangle_Z \\ &= \langle x_f, \mathcal{T}^*\mathcal{P}\mathcal{A}x_f\rangle_Z + \langle x_f, \mathcal{A}^*\mathcal{P}\mathcal{T}x_f\rangle_Z \\ &= \langle x_f, (\mathcal{T}^*\mathcal{P}\mathcal{A} + \mathcal{A}^*\mathcal{P}\mathcal{T})x_f\rangle_Z. \end{aligned} \quad (24)$$

Based on (19), the PI operator $\mathcal{A}$ with uncertainties satisfies the following condition:

$$\mathcal{A} = \mathcal{A}_1 + g(t)\mathcal{A}_2 \quad (25)$$

where

$$\mathcal{A}_1 = \mathcal{P}\begin{bmatrix} \bar{A}_0 & \bar{A}_1 \\ 0 & \{\Upsilon,0,0\} \end{bmatrix}, \ \mathcal{A}_2 = \mathcal{P}\begin{bmatrix} \Delta\bar{A}_0 & \Delta\bar{A}_1 \\ 0 & \{0,0,0\} \end{bmatrix}_{g(t)=1}.$$

Obviously, $\mathcal{A}$ is consequently convex with respect to $\mathcal{A}_1$ and $\mathcal{A}_2$. $\dot{V}(x_f) \leq 0$ holds if there exists a PI operator $\mathcal{P}$ satisfying the condition (22) for $g(t) \in \{0, 1\}$. In summary, if condition (22) holds, the multiarea LFC system with EVs and time delays is asymptotically stable. This completes the proof. ■

According to Theorem 1, if the PI operator $\mathcal{A}$ does not contain uncertainties, the following corollary can be obtained.

Corollary 1: For given time delays $\tau_i (i = 0, 1, \ldots, N)$, the system (19) without uncertainties is asymptotically stable if there exist a positive, self-adjoint PI operator $\mathcal{P} := \mathcal{P}\begin{bmatrix} P, & Q_1 \\ Q_2, & \{R_i\} \end{bmatrix}$ such that the following inequality holds:

$$\mathcal{T}^*\mathcal{P}\mathcal{A} + \mathcal{A}^*\mathcal{P}\mathcal{T} < 0. \quad (26)$$

Remark 4: Note that Theorem 1 is suitable for multiarea LFC system with EVs and time delays. When the multiarea LFC system includes EVs without SOC or does not include EVs, Corollary 1 is applicable. Compared with the results of [13] and [26], Theorem 1 and Corollary 1 are more concise and understandable thanks to the PIE representation.

Remark 5: The integral inequality technique is obviously not utilized in the proof of Theorem 1. Instead, it needs to be introduced to deal with the cross term of the derivative of simple L–K functional in time domain indirect approach (see [10], [13], [18], [21]–[23], [25], and [26]). Not that the integral inequality is an approximation of the cross-term, which inevitably increases conservatism of the criteria.

TABLE I
PARAMETERS OF TWO-AREA LFC SYSTEM

	T_{ti}	T_{gi}	R_i	D_i	β_i	M_i	T_{12}
Area 1	0.3	0.1	0.05	1	21	10	0.1986
Area 2	0.4	0.17	0.05	1.5	21.5	12	0.1986

Therefore, the stability criteria proposed in this article are less conservative.

Remark 6: According to Lemma 1, the PI operator can be parameterized by utilizing matrix valued functions, so PI operator inequality can be converted into a series of LMIs. Furthermore, PIETOOLS provides a good interface to construct and parameterize the PI operator. Therefore, the operator inequality (22) can be efficiently calculated by PIETOOLS. It is easy to calculate the delay margins of multiarea LFC system with EVs and time delays based on the method proposed in this article.

The procedures for calculating the delay margin are provided as follows.

Step 1: Acquiring the dynamical model of the LFC system. By analyzing system components (such as non-reheat turbines), the corresponding system model parameters can be obtained.

Step 2: Establishing the closed-loop system. First, the LFC scheme with PID controller can be expressed by DDEs. Then, the system represented by DDEs is transformed to one by PIE based on PI operator.

Step 3: Calculating the delay margins. Based on Theorem 1, the operator inequality constraints are established in PIETOOLS, and the delay margins of the LFC system are obtained by using the binary search method.

Step 4: Simulating the LFC system with time delays. Simulation results are utilized to verify the accuracy of the delay margins.

IV. CASE STUDIES

In this section, case studies are implemented to illustrate the effectiveness and advantages of the proposed method. The detailed system parameters are used in [21], [22], and [26] and recorded in Table I. The delay margins calculated by Theorem 1 and Corollary 1 are compared with other different method in this section. Then, simulation studies of the one-area and two-area LFC system are carried out to verify the validity of the approach.

A. One-Area LFC Scheme

Numerical examples and simulations for one-area LFC system with time delay are provided in this section.

Case 1: A one-area LFC system with time delay is investigated in which the EVs are not integrated. The system dynamics model are given in [22], and the system parameters are shown in area 1 of Table I. Delay margins of a one-area LFC with PI controller ($K_P, K_I \in 0.1, 0.2, 0.4, 0.6, 0.8$) are obtained based on Corollary 1. The results are recorded in Table II along with the ones given in [22]. Note that the

TABLE II
DELAY MARGINS FOR ONE-AREA LFC SYSTEM WITHOUT EVS

K_P	K_I	[22]	Cor. 1	K_P	K_I	[22]	Cor. 1
0.10	0.05	31.61	32.75	0.60	0.10	12.30	17.19
0.20	0.05	30.39	34.22	0.60	0.15	8.94	11.27
0.40	0.05	26.38	35.83	0.60	0.20	7.05	8.31
0.60	0.05	20.69	34.92	0.60	0.40	3.66	3.82
0.10	0.10	16.02	16.11	0.80	0.05	14.67	29.44
0.20	0.10	16.43	16.85	0.80	0.15	6.57	9.39
0.40	0.10	15.09	17.65	0.80	0.20	5.18	6.86
0.80	0.10	8.92	14.29	0.80	0.40	2.61	2.91

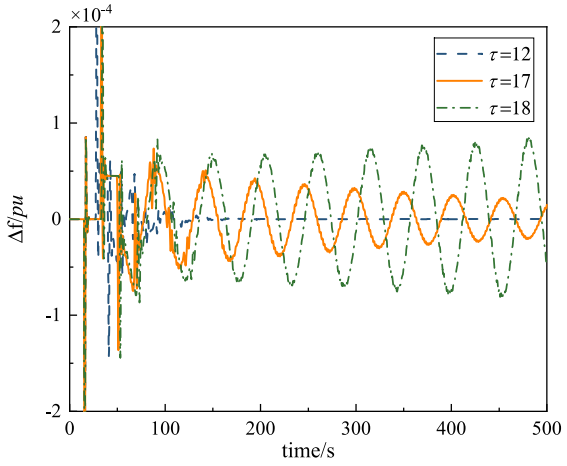

Fig. 2. Response of Δf for one-area LFC system without EVs.

delay margins calculated by Corollary 1 are larger than the results obtained in [22] based on Table II. The delay margins obtained by the approach in this article is very close to the result obtained by the frequency domain method (error less than 0.01), but the frequency domain method may be not suitable for multiarea LFC system with EVs. It clearly shows that the proposed method is less conservative.

Simulation tests are conducted to validate the accuracy of delay margin, which is calculated by the proposed approach. The simulation results of the one-area LFC system with PI controller ($K_P = 0.6, K_I = 0.1$) are conducted. According to [10], the update period of area control error $ACE(t)$ signal is set to 2 s. The initial value of the one-area LFC system is 0, and a step load disturbance ($\Delta P_{di} = 0.1pu$) occurs at t = 15 s. From Table II, the delay margins computed by Corollary 1 and [22] are 12.30 and 17.19 when $K_P = 0.6$ and $K_I = 0.1$, respectively. Then, the responses of the state Δf for different delay margins ($\tau = 12$, $\tau = 17$, and $\tau = 18$) are displayed in Fig. 2. It is clear that the one-area LFC system is stable when $\tau = 12$ and $\tau = 17$, but when $\tau = 18$, the LFC system is unstable. This simulation tests reveal that the stability criteria given in this article are efficient.

Case 2: A one-area LFC system with EVs and time delays is studied in this case. The system parameters are selected from [4] as $\bar{K}_e = 1$, $T_e = 1$, $\alpha_1 = 0.8$, $\alpha_2 = 0.2$, $\rho_e = 1/R_g$, and $\lambda = 0.8$. Based on Theorem 1, the delay margins of the one-area LFC system with EVs are derived ($K_P, K_I \in 0.1, 0.2, 0.4, 0.6, 0.8$). Table III shows the delay margins of the LFC system with and without EVs under the same controller

TABLE III
DELAY MARGINS FOR ONE-AREA LFC SYSTEM WITH EVS

K_P	K_I	Case 1	Case 2	K_P	K_I	Case 1	Case 2
0.10	0.05	32.75	44.86	0.60	0.10	17.19	25.06
0.20	0.05	34.22	46.53	0.60	0.15	11.27	16.61
0.40	0.05	35.83	49.09	0.60	0.20	8.31	12.37
0.60	0.05	34.92	50.35	0.60	0.40	3.82	5.96
0.10	0.10	16.11	22.32	0.80	0.05	29.44	49.8
0.20	0.10	16.85	23.15	0.80	0.15	9.39	16.41
0.40	0.10	17.65	24.43	0.80	0.20	6.86	12.21
0.80	0.10	14.29	24.78	0.80	0.40	2.91	5.82

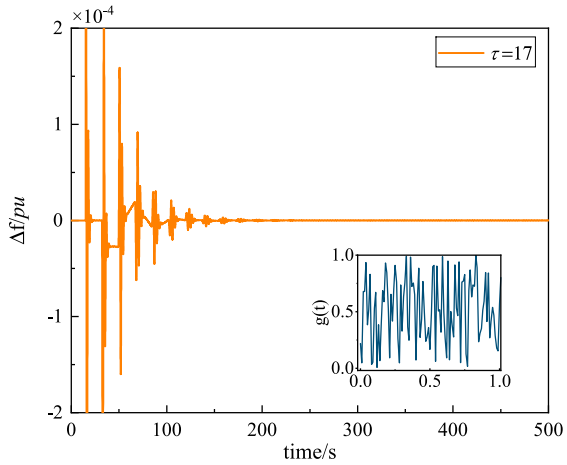

Fig. 3. Response of Δf for one-area LFC system with EVs.

TABLE IV
DELAY MARGINS FOR TWO-AREA LFC SYSTEM WITHOUT EVS

θ	[33](error)	[21](error)	[26] (error)	The. 1(error)	Simulation
0°	4.86(42.34%)	5.36(36.41%)	7.59(9.96%)	8.43(0%)	8.43
20°	4.78(46.71%)	5.97(33.44%)	8.65(3.56%)	8.95(0.22%)	8.97
40°	5.71(48.13%)	7.19(34.69%)	10.97(0.36%)	11.00(0.09%)	11.01
50°	5.97(46.45%)	7.17(35.69%)	11.11(0.35%)	11.14(0.08%)	11.15
70°	4.93(45.76%)	5.96(34.43%)	8.73(3.96%)	9.00(0.99%)	9.09
90°	4.89(42.74%)	5.35(37.35%)	7.53(11.82%)	8.54(0%)	8.54

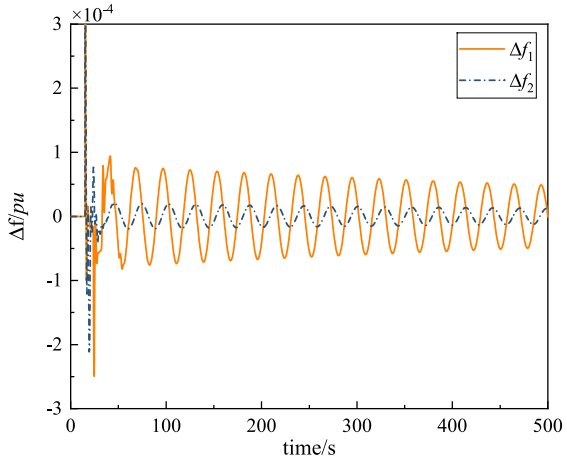

Fig. 4. Response of Δf for two-area LFC system without EVs.

parameters. Obviously, the integration of EVs increases the delay margins of the LFC system. It is shown that EVs can help the LFC system resist performance degradation caused by time delay. Moreover, the insertion of EVs may not affect the relationship between the delay margins and the controller parameters.

The simulation results of the one-area LFC system with EVs are given to illustrate the effectiveness of the method. $g(t)$ is selected as a random number between 0 and 1 as shown in Fig. 3. The controller parameters and time delay are set to the same as in case 1($K_P = 0.6, K_I = 0.1, \tau = 17$). Then, the state responses of the one-area LFC system with EVs are obtained. Fig. 3 shows the response of the deviation of frequency Δf. By comparing with Fig. 2, the frequency error of the LFC system with EVs can converge to a steady state in a short time. It indicates that the integration of EVs can help power plants suppress frequency changes and improve system performance.

B. Two-Area LFC Scheme

The delay margins of a two-area LFC system with or without EVs both be obtained in this section. For comparison, the controller parameters of each control area are considered to be equal.

Case 3: A two-area LFC system with time delays is considered in this case which is more comprehensive and practical. The delay margins for two-area LFC system with time delays are computed by Corollary 1. For $K_P = 0.4$ and $K_I = 0.2$, the results of this article are recorded in Table IV along with the results given in [21], [26], and [33]. A polar representation is used in Table IV, in which $\theta = \tan^{-1}(\tau_1/\tau_2)$ and $\tau = \sqrt{\tau_1^2 + \tau_2^2}$ represent angle and magnitude, respectively. By setting the initial states of the two-area LFC system to arbitrary values, the simulated values are shown in Table IV. According to Table IV, the errors between delay margins obtained in this article and the simulated values are always less than 1%. However, the maximum errors between the results of [21], [26], and [33] and the simulated values are 11.82%, 37.35%, and 48.18%, respectively. The error varies with θ. It is mean that the delay margins obtained by the operator method are nearly accurate. Therefore, the method proposed in this article is effective for multiarea LFC system with time delays.

The simulation results of the two-area LFC system with ($K_P = 0.4$, $K_I = 0.2$ and $\tau = 9.00, \theta = 70°$) are given in this section. The initial values of the two-area LFC system are set to 0, and a step load disturbance ($\Delta P_{di} = 0.1$ pu) is implemented at $t = 15$ s. When $\tau = 9.00$ and $\theta = 70°$, the time delays of two areas are $\tau_1 = 8.45$ and $\tau_2 = 3.07$, respectively. Fig. 4 shows the state responses of Δf_1 and Δf_2. It is obvious that the two-area LFC system is asymptotically stable, which validate the effectiveness of the method in this article.

Case 4: The delay margins of a two-area LFC system with EVs and time delays are computed. The parameters of EV in two areas are set to be the same as in case 2. Based on Theorem 1, the delay margins of the two-area LFC system with EVs and time delays are derived($K_P = 0.4, K_I = 0.2$). Table V shows the delay margins obtained in cases 3 and 4. Compared with the one-area LFC system, the integration of

TABLE V
DELAY MARGINS FOR TWO-AREA LFC SYSTEM WITH EVS

θ	[25]	Case 3	Case 4
0°	7.59	8.43	9.95
20°	8.65	8.95	10.55
40°	10.97	11.00	13.43
50°	11.11	11.14	13.40
70°	8.73	9.00	10.23
90°	7.53	8.54	9.89

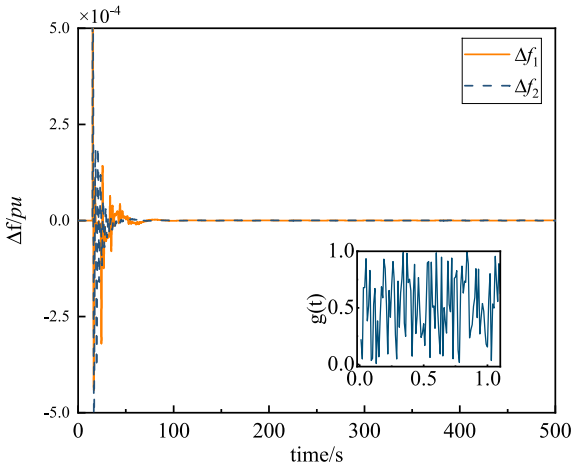

Fig. 5. Response of Δf_i of two-area LFC system with EVs.

EVs has less effect on the delay margin of multiarea LFC system. The method proposed in this article is effective for multiarea LFC system with EVs and time delays.

The simulation results of the two-area LFC system with EVs and time delays are given to illustrate the significance of EVs. Fig. 5 shows the responses of Δf_1 and Δf_2 under the same parameters as case 3 ($K_P = 0.4$, $K_I = 0.2$ $\tau_1 = 8.45$, and $\tau_2 = 3.07$). The system reached steady state before 100 s according to Fig. 5. It indicate that the access of EVs can significantly improve the performance of the multiarea LFC system with time delays.

V. CONCLUSION

This article has studied the problem of stability analysis of multiarea LFC system with EVs and time delays. In order to reduce the conservativeness caused by time-domain method, the multiarea LFC system with EVs and time delays is represented by PIE for the first time in this article. Moreover, the complete quadratic L–K functional is built, which is more general than simple L–K functional. The novel stability results with less conservatism are obtained in the form of the operator inequality and some novel interactions between delay margins and controller parameters are discovered. Finally, case studies are given to verify the superiority of the proposed approach.

REFERENCES

[1] P. Kundur, N. J. Balu, and M. G. Lauby, *Power System Stability and Control*. vol. 7. New York, NY, USA: McGraw-Hill, 1994.

[2] H. Sun, C. Peng, D. Yue, Y. L. Wang, and T. Zhang, "Resilient load frequency control of cyber-physical power systems under qos-dependent event-triggered communication," *IEEE Trans. Syst., Man, Cybern., Syst.*, early access, Mar. 27, 2020, doi: 10.1109/TSMC.2020.2979992.

[3] Z. Hu, S. Liu, W. Luo, and L. Wu, "Resilient distributed fuzzy load frequency regulation for power systems under cross-layer random denial-of-service attacks," *IEEE Trans. Cybern.*, early access, Jul. 22, 2020, doi: 10.1109/TCYB.2020.3005283.

[4] T. N. Pham, S. Nahavandi, L. V. Hien, H. Trinh, and K. P. Wong, "Static output feedback frequency stabilization of time-delay power systems with coordinated electric vehicles state of charge control," *IEEE Trans. Power Syst.*, vol. 32, no. 5, pp. 3862–3874, Sep. 2017.

[5] E. Tian and C. Peng, "Memory-based event-triggering H_∞ load frequency control for power systems under deception attacks," *IEEE Trans. Cybern.*, vol. 50, no. 11, pp. 4610–4618, Nov. 2020.

[6] S. Saxena and E. Fridman, "Event-triggered load frequency control via switching approach," *IEEE Trans. Power Syst.*, vol. 35, no. 6, pp. 4484–4494, Nov. 2020.

[7] A. Naveed, Ş. Sönmez, and S. Ayasun, "Impact of electric vehicle aggregator with communication time delay on stability regions and stability delay margins in load frequency control system," *J. Mod. Power Syst. Clean Energy*, to be published, doi: 10.35833/MPCE.2019.000244.

[8] Q. Zhu, L. Jiang, W. Yao, C. K. Zhang, and C. Luo, "Robust load frequency control with dynamic demand response for deregulated power systems considering communication delays," *Elect. Power Compon. Syst.*, vol. 45, no. 1, pp. 75–87, 2017.

[9] A. Mohanty, M. Viswavandya, P. K. Ray, S. Mohanty, and P. P. Mohanty, "Linear matrix inequality approach in stability improvement through reactive power control in hybrid distributed generation system," *IET Smart Grid*, vol. 2, no. 3, pp. 355–363, 2019.

[10] C. Zhang, L. Jiang, Q. Wu, Y. He, and M. Wu, "Delay dependent robust load frequency control for time delay power systems," *IEEE Trans. Power Syst.*, vol. 28, no. 3, pp. 2192–2201, Aug. 2013.

[11] C. Peng and J. Zhang, "Delay-distribution-dependent load frequency control of power systems with probabilistic interval delays," *IEEE Trans. Power Syst.*, vol. 31, no. 4, pp. 3309–3317, Jul. 2016.

[12] P. Ojaghi and M. Rahmani, "LMI-based robust predictive load frequency control for power systems with communication delays," *IEEE Trans. Power Syst.*, vol. 32, no. 5, pp. 4091–4100, Sep. 2017.

[13] F. Yang, J. He, and Q. Pan, "Further improvement on delay-dependent load frequency control of power systems via truncated B-L inequality," *IEEE Trans. Power Syst.*, vol. 33, no. 5, pp. 5062–5071, Sep. 2018.

[14] X. ShangGuan, Y. He, C. Zhang, L. Jiang, J. W. Spencer, and M. Wu, "Sampled-data based discrete and fast load frequency control for power systems with wind power," *Appl. Energy*, vol. 259, Feb. 2020, Art. no. 114202.

[15] S. Weng, D. Yue, C. Dou, J. Shi, and C. Huang, "Distributed event-triggered cooperative control for frequency and voltage stability and power sharing in isolated inverter-based microgrid," *IEEE Trans. Cybern.*, vol. 49, no. 4, pp. 1427–1439, Apr. 2019.

[16] S. Sönmez, A. Saffet, and C. O. Nwankpa, "An exact method for computing delay margin for stability of load frequency control systems with constant communication delays," *IEEE Trans. Power Syst.*, vol. 31, no. 1, pp. 370–377, Jan. 2016.

[17] S. Sönmez and S. Ayasun, "Stability region in the parameter space of Pi controller for a single-area load frequency control system with time delay," *IEEE Trans. Power Syst.*, vol. 31, no. 1, pp. 829–830, Jan. 2016.

[18] L. Jiang, W. Yao, Q. H. Wu, J. Y. Wen, and S. J. Cheng, "Delay-dependent stability for load frequency control with constant and time-varying delays," *IEEE Trans. Power Syst.*, vol. 27, no. 2, pp. 932–941, May 2012.

[19] C. Hua, Y. Wang, and S. Wu, "Stability analysis of neural networks with time-varying delay using a new augmented Lyapunov–Krasovskii functional," *Neurocomputing*, vol. 332, pp. 1–9, Mar. 2019.

[20] K. Shi, H. Zhu, S. Zhong, Y. Zeng, Y. Zhang, and W. Wang, "Stability analysis of neutral type neural networks with mixed time-varying delays using triple-integral and delay-partitioning methods," *ISA Trans.*, vol. 58, pp. 85–95, Sep. 2015.

[21] C. Zhang, L. Jiang, Q. H. Wu, Y. He, and M. Wu, "Further results on delay-dependent stability of multi-area load frequency control," *IEEE Trans. Power Syst.*, vol. 28, no. 4, pp. 4465–4474, Nov. 2013.

[22] F. Yang, J. He, and D. Wang, "New stability criteria of delayed load frequency control systems via infinite-series-based inequality," *IEEE Trans. Ind. Informat.*, vol. 14, no. 1, pp. 231–240, Jan. 2018.

[23] F. Yang, J. He, J. Wang, and M. Wang, "Auxiliary-function-based double integral inequality approach to stability analysis of load frequency control systems with interval time-varying delay," *IET Control Theory Appl.*, vol. 12, no. 5, pp. 601–612, Mar. 2017.
[24] K. Ramakrishnan and G. Ray, "Stability criteria for nonlinearly perturbed load frequency systems with time-delay," *IEEE J. Emerg. Sel. Topics Circuits Syst.*, vol. 5, no. 3, pp. 383–392, Sep. 2015.
[25] H. Luo, I. A. Hiskens, and Z. Hu, "Stability analysis of load frequency control systems with sampling and transmission delay," *IEEE Trans. Power Syst.*, vol. 35, no. 5, pp. 3603–3615, Sep. 2020.
[26] L. Jin, C.-K. Zhang, Y. He, L. Jiang, and M. Wu, "Delay-dependent stability analysis of multi-area load frequency control with enhanced accuracy and computation efficiency," *IEEE Trans. Power Syst.*, vol. 34, no. 5, pp. 3687–3696, Sep. 2019.
[27] C. Hua, Y. Wang, and S. Wu, "Stability analysis of micro-grid frequency control system with two additive time-varying delay," *J. Franklin Inst.*, vol. 357, no. 8, pp. 4949–4963, 2020.
[28] M. M. Peet, "A new state-space representation for coupled PDEs and scalable lyapunov stability analysis in the SOS framework," in *Proc. IEEE Conf. Decis. Control*, 2018, pp. 545–550.
[29] S. Shivakumar, A. Das, and M. M. Peet, "PIETOOLS: A MATLAB toolbox for manipulation and optimization of partial integral operators," in *Proc. Amer. Control Conf. (ACC)*, 2020, pp. 2667–2672.
[30] S. Wu, M. M. Peet, and C. Hua, "Estimator-based output-feedback stabilization of linear multi-delay systems using SOS," in *Proc. IEEE Conf. Decis. Control (CDC)*, 2019, pp. 983–988.
[31] M. M. Peet, "A dual to Lyapunov's second method for linear systems with multiple delays and implementation using SOS," *IEEE Trans. Autom. Control*, vol. 64, no. 3, pp. 944–959, Mar. 2019.
[32] S. Shivakumar and M. M. Peet, "Computing input–ouput properties of coupled linear PDE systems," in *Proc. Amer. Control Conf. (ACC)*, 2019, pp. 606–613.
[33] X. Yu, H. Jia, and C. Wang, "CTDAE & CTODE models and their applications to power system stability analysis with time delays," *Sci. China Technol. Sci.*, vol. 56, no. 5, pp. 1213–1223, 2013.

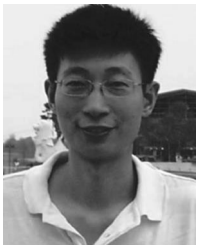

Changchun Hua (Senior Member, IEEE) received the Ph.D. degree in electrical engineering from Yanshan University, Qinhuangdao, China, in 2005.

He was a Research Fellow with the National University of Singapore, Singapore, from 2006 to 2007. From 2007 to 2009, he worked with Carleton University, Ottawa, ON, Canada, funded by Province of Ontario Ministry of Research and Innovation Program. From 2009 to 2010, he worked with the University of Duisburg–Essen, Duisburg, Germany, funded by Alexander von Humboldt Foundation. He is currently a Full Professor with Yanshan University, Qinhuangdao, China. He has authored or coauthored of more than 120 papers in mathematical, technical journals, and conferences. He has been involved in more than 15 projects supported by the National Natural Science Foundation of China, the National Education Committee Foundation of China, and other important foundations. He is Cheung Kong Scholars Programme Special appointment professor. His research interests are in nonlinear control systems, multiagent systems, control systems design over network, teleoperation systems, and intelligent control.

Yibo Wang received the B.S. degree in electrical engineering from Bohai University, Jinzhou, China, in 2017. He is currently pursuing the Ph.D. degree with Yanshan University, Qinhuangdao, China.

His current research interests include power systems, time-delay systems, and networked control systems.